AN IMPROVED STRIP THEORY PROGRAM FOR SHIP MOTIONS AND SEA LOADS IN WAVES

Kevin McTaggart, Defence Research Establishment Atlantic, P.O. Box 1012, Dartmouth, Nova Scotia, B2Y 3Z7

Abstract

This paper describes enhancements to the strip theory program SHIPMO. The goal of recent development work was to produce a robust code for predicting both ship motions and sea loads in waves. A new boundary element method eliminates irregular frequencies of sectional hydrodynamic coefficients. Problems with predictions at low encounter frequencies are circumvented with a new extrapolation scheme. These improvements remove two sources of potentially large errors for predicted motions and sea loads. A new added resistance capability uses two different near-field methods for short and long wavelength regimes. Motion and sea load predictions include appendage and viscous forces for the lateral plane. Validation results for a warship indicate good agreement of predicted motions and sea loads with experiments.

NOMENCLATURE

A_{ij}	added mass
a_{ij}	sectional added mass
B	ship beam
B_{ij}	damping
C_B	ship block coefficient
C_{ij}	stiffness
D_i^x	hydrodynamic load at x for mode i
Fn	Froude number
F_i^x	wave excitation load at x for mode i
$\overline{GM}$	metacentric height
g	gravitational acceleration
h	steady wave elevation
I_i^x	inertial load at x for mode i
I_{ij}	ship dry inertia
k	wavenumber
k_r	roll inertia proportionality constant
L	ship length
l_i	length of segment i
m_i	mass of segment i
p	hydrodynamic pressure
N_s	number of ship segments
n_x	x component of normal vector
p	hydrodynamic pressure
R_{AW}	added resistance in waves
R_{AW}^{lw}	added resistance in long waves
R_{AW}^{sw}	added resistance in short waves
R'_{AW}	added resistance in unit amplitude waves
R_i^x	hydrodynamic reaction load at x for mode i
r_{ij}	ship dry radius of gyration
r_{xx-i}	local roll radius of gyration
S	ship surface
$S_{\beta_s,\omega}(\beta_s,\omega)$	directional wave spectral density
T	ship draft
U	ship speed
V_i^x	total load at x for mode i
wl	ship waterline
wl^*	waterline exposed to incident waves
x, y, z	ship coordinate system
y_{max}	maximum y coordinate of section
z_i	centre of gravity elevation of segment i
β_s	sea direction
ζ_D	diffracted wave amplitude
ζ_I	incident wave amplitude
ζ_i	motion for mode i
ζ_r	relative motion
θ	horizontal angle of ship waterline relative to incident wave direction
λ	wavelength
ρ	water density
ω	wave frequency
ω_e	wave encounter frequency
ω_{e-o}	encounter frequency lower limit
ω_4	wet roll natural frequency
$\triangle$	ship mass displacement

INTRODUCTION

Predictions of motions and sea loads in waves have become integral elements of modern ship design. Strip theory frequency domain codes, based largely on the work of Salvesen, Tuck, and Faltinsen [1], are the most popular tools for predicting ship motions and sea loads. Although more sophisticated three-dimensional and time domain methods are available, strip theory remains popular because it is computationally efficient, robust, and sufficiently accurate in most cases. Despite slenderness assumptions, strip theory can give good ship motion predictions for length/beam ratios as low as $L/B = 4$ [2]. Ongoing work at DREA indicates that strip theory will give good results for Froude numbers up to 0.4 and in wave conditions up to Sea State 7 for naval frigates. In general, the limitations of strip theory are acceptable.

This paper describes the latest version of DREA's strip theory program SHIPMO. The original program, which was developed in the late 1970's, was based on Salvesen, Tuck, and Faltinsen's theory, with enhancements by Schmitke [3] to include appendage and viscous forces, which significantly influence motions in the lateral plane. Subsequent improvements included more sophisticated roll damping computations, including Himeno's method [4] for eddy roll damping. The latest version of SHIPMO was developed to produce a robust and accurate design tool for predicting sea loads in waves. Improved methods for determining sectional hydrodynamic coefficients eliminate irregular frequencies, a common source of errors in hydrodynamic codes. To avoid problems with strip theory computations at low encounter frequencies, an approximate method utilizes ship motion and sea load predictions at higher encounter frequencies. Added resistance in waves is evaluated using a near-field method, which gives more reliable results than far-field methods which are often used in strip theory codes. A carefully implemented sea load prediction capability gives good load predictions in both the vertical and lateral planes.

Figure 1 shows the ship axis system, which is used for all equations in this paper. The axis origin is at the ship centre of gravity. Figure 2 shows the sea direction definition, with $\beta_s = 0$ for following seas. Ship stations are numbered with station 0 at the forward perpendicular and station 20 at the aft perpendicular.

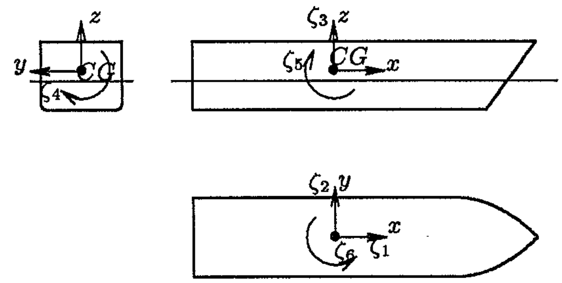

Figure 1: SHIPMO Ship Axes

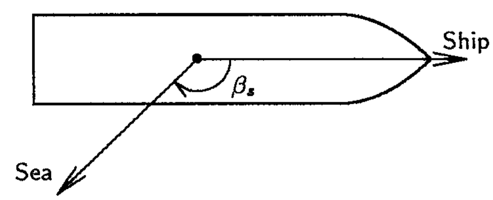

Figure 2: Sea Direction

SECTIONAL HYDRODYNAMIC COEFFICIENTS

Evaluation of sectional hydrodynamic coefficients is one of the primary computational tasks in strip theory. The Frank close-fit method [5] has been commonly used by strip theory codes. Although it is efficient, the Frank close-fit method has two problems that can adversely influence ship motion predictions. First, the method can produce severe errors for sections with horizontal or vertical line segments. This problem is sometimes countered by slight adjustments to the orientation of horizontal or vertical segments. Second, the method suffers from irregular frequencies for surface-piercing sections. An irregular frequency is a frequency at which a numerical solution exists that does not reflect physical reality, but instead represents a standing wave within the ship section. Figure 3 gives heave added mass for a ship transom section with an irregular frequency of 3.4 rad/s. Irregular frequencies generally occur at the higher end of the frequency range for ship motions.

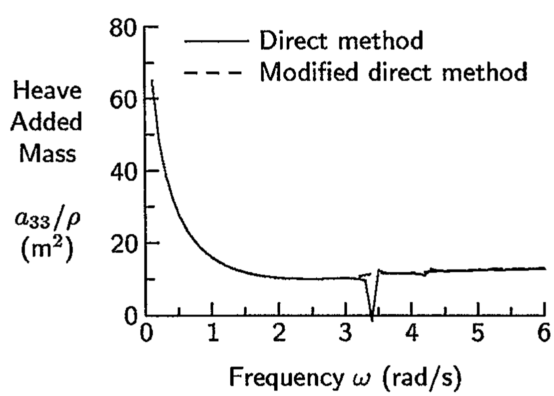

Figure 3: Heave Added Mass for Transom Section

When predicting ship motions, irregular frequencies do not usually create severe errors because hydrodynamic forces are integrated over a large number of sections, thus minimizing irregular frequency effects which might typically occur at only one or two ship sections for a given wave frequency. In contrast to ship motions, irregular frequencies can cause much greater problems for sea loads because local forces are integrated over a smaller number of sections.

Elimination of Irregular Frequencies

As stated earlier, irregular frequencies are caused by mathematical solutions that induce standing waves within a surface-piercing ship section. The new version of SHIPMO replaces the Frank close-fit method with a boundary element method from Sclavounos and Lee [6]. The implementation uses algorithms from Newman [7] for computing the Green function. For calculating velocity potentials and resulting hydrodynamic coefficients, Sclavounos and Lee describe a direct method and an improved direct method which practically eliminates irregular frequencies. The improved direct method implemented in SHIPMO requires more computational effort than the Frank close-fit method; however, the new method has no practical restrictions on geometries and still has very acceptable computational requirements. The heave added masses shown in Figure 3 demonstrate the effectiveness of the modified direct method for eliminating irregular frequencies for heave added mass. The modified direct method is similarly effective for sway and roll sectional coefficients.

Approximations at Zero and Infinite Frequencies

Before computing ship motions, a strip theory code typically computes and stores sectional hydrodynamic coefficients for a limited range of encounter frequencies. When computing ship motions, the code then uses interpolation of the stored hydrodynamic coefficients to obtain coefficients as required. In the new version of SHIPMO, hydrodynamic coefficients can be obtained at frequencies outside the range of stored coefficient values using approximations based on zero and infinite frequency coefficients.

For a body oscillating in water, the waves radiated by the body will approach zero amplitude as the oscillation frequency approaches zero or infinity; thus, radiation damping becomes zero as frequency approaches zero or infinity.

At high frequencies, the sectional added masses for sway, heave, and roll approach their infinite frequency values. SHIPMO uses this approximation for added masses at high encounter frequencies. For sway at low encounter frequency, sectional added mass is approximated by the zero frequency value. For heave and roll of two-dimensional surface-piercing sections, Newman [8] states that the mathematical solution of the flow becomes invalid as encounter frequency approaches zero, as demonstrated in Figure 3 by the unrealistic trend of heave added mass going to infinity at zero frequency. Strip theory computations of heave added mass for slender ellipsoids indicate that sectional added mass at frequency $0.2\sqrt{g/y_{max}}$ provides a reasonable approximation for heave added mass at lower frequencies, with y_{max} being the maximum lateral offset of a section. Figure 4 show three-dimensional computations from Kim [9] and from strip theory for a semi-submerged ellipsoid with $L/B = 8$. The ellipsoid results demonstrate that strip theory requires the low frequency correction to give reasonable results for heave added mass. For roll added mass, predicted values are generally constant at low frequencies even though the theoretical formulation becomes invalid at zero frequency. In SHIPMO, the roll added mass computed at the lowest encounter frequency for stored coefficients is used for lower encounter frequencies.

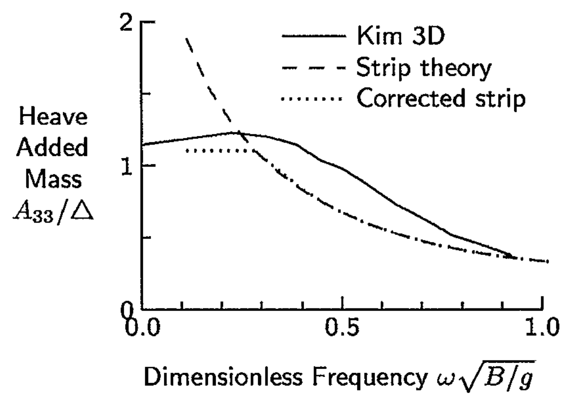

Figure 4: Ellipsoid Heave Added Mass, $L/B = 8$

MOTIONS AND LOADS AT LOW ENCOUNTER FREQUENCIES

A ship in regular waves experiences motions and sea loads at the wave encounter frequency given by:

$$\omega_e = |\omega - k\,U\,\cos\beta_s| \qquad (1)$$

where ω is wave frequency, k is wavenumber, and β_s is the sea direction relative to the ship forward speed (see Figure 2). SHIPMO assumes all computations are for deep water, giving the following relationship between wavenumber and wave frequency:

$$k = \frac{\omega^2}{g} \qquad (2)$$

In following seas ($|\beta_s| < 90$ degrees), the encounter frequency can go to zero at non-zero wave frequencies, as demonstrated in Figure 5 for a heading of 30 degrees and Froude number of 0.29. Strip theory predictions of hydrodynamic coefficients and forces deteriorate as encounter frequency approaches zero because of inherent limitations in the theory. The absence of restraining forces in surge, sway, and yaw also causes problems with motion predictions at low encounter frequencies.

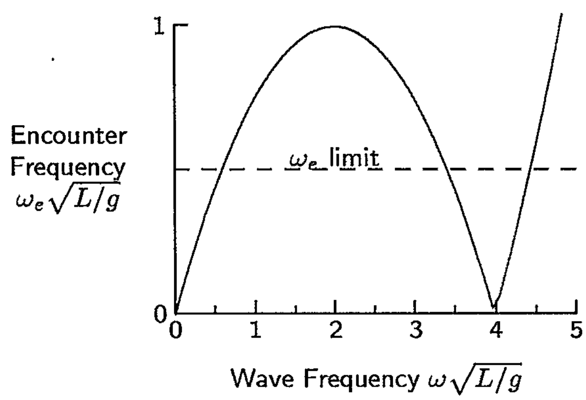

Figure 5: Encounter Frequencies for Heading = 30 degrees, $Fn = 0.29$

Experience with SHIPMO shows that strip theory gives reliable predictions at encounter frequencies above the following limiting value:

$$\omega_{e-o} = 0.5\sqrt{\frac{g}{L}} \qquad (3)$$

If a wave frequency ω gives an encounter frequency lower than ω_{e-o}, then the motions and loads are extrapolated from values at wave frequencies with encounter frequencies equal to or greater than ω_{e-o}. At low encounter frequencies, all complex values of sea loads and translational motions (surge, sway, and heave) are assumed to be linear functions of wave frequency, while complex values of rotational motions (roll, pitch, yaw, rudder, and stabilizer fins or tank) divided by wavenumber k are assumed to be linear functions of wave frequency. This extrapolation scheme requires motion predictions to include wave frequencies with encounter frequencies equal to or greater than ω_{e-o}.

Figure 6 shows predicted sway motions for the warship model of References 10 and 11 with and without correction of motions at low encounter frequencies. The absence of restoring forces in surge, sway, and yaw can cause unrealistically high motion predictions at low encounter frequencies. For heave, roll, and pitch, predictions at low encounter frequencies are plagued by errors in computed hydrodynamic coefficients. The approximation described in the previous paragraph gives reliable results at low encounter frequencies and avoids potentially severe errors of strip theory.

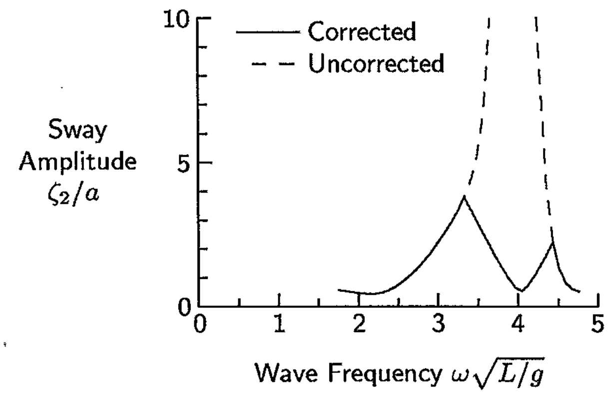

Figure 6: Predicted Sway of Warship Model, Heading = 30 degrees, $Fn = 0.29$

ADDED RESISTANCE IN WAVES

For a ship travelling at a given speed, the resistance in a seaway will usually be greater than the calm water resistance due to added resistance in waves. Added resistance is the mean value of along-ship forces due to waves and resulting motions.

Added resistance has practical implications for ship design and operation. If a ship must be designed to achieve a given speed in a seaway, then its propulsion capacity must include a margin for added resistance. Conversely, a ship with no margin for added resistance will have reduced speed capability in a seaway. Increased power requirements from added resistance will also reduce cavitation inception speed, which can be particularly important for naval vessels.

Added Resistance Theory

Added resistance can be predicted using either a near-field or a far-field method. A far-field method, such as Salvesen's [12], considers the energy radiated from the ship as it moves in waves. Alternatively, a near-field method directly predicts the mean forces acting on the ship as follows:

$$R_{AW} = -\int_S \overline{p\, n_x}\, dS \qquad (4)$$

where S is the wetted surface of the ship, p is hydrodynamic pressure, and n_x is the x component of the normal vector pointing into the ship. The line over $p\ n_x$ indicates the time average. In practice, the above equation must be evaluated very carefully because the terms within the integral tend to nullify each other, with added resistance being the final residual.

References 13 and 14 indicate that the dominant term in the near-field method is the following integral taken about the ship waterline:

$$R_{AW} = -\frac{\rho\, g}{2} \int_{wl} \overline{\zeta_r^2(x,y,t)\, n_x}\, dl \qquad (5)$$

where wl is the ship waterline and $\zeta_r(x,y,t)$ is the relative motion. Neglecting the effect of dynamic swell-up due to ship forward speed, the relative motion amplitude can be expressed as:

$$\zeta_r = \zeta_I + \zeta_D - \zeta_3 - y\zeta_4 + x\zeta_5 \qquad (6)$$

where ζ_I is the incident wave elevation, ζ_D is the diffracted wave elevation, ζ_3 is ship heave, ζ_4 is ship roll, and ζ_5 is ship pitch. Blok and Huisman [15] state that the relative motion can be re-written to include the effect of swell-up due to forward ship speed as follows:

$$\zeta_r = \left(1 + \frac{\partial h(x,U)}{\partial T}\right) \times (\zeta_I + \zeta_D - \zeta_3 - y\zeta_4 + x\zeta_5) \qquad (7)$$

where $h(x,U)$ is the steady wave elevation along the ship due to forward speed and T is ship draft.

The greatest problem in applying Equation (5) to predicting added resistance is that strip theory cannot evaluate the diffracted wave elevation ζ_D. Fortunately, Reference 13 gives two different near-field equations for determining added resistance within this limitation of strip theory. When wavelength is of the order of ship length or greater, ship motions will be significant but diffraction effects will be negligible (i.e. $\zeta_D \approx 0$). The added resistance in long waves will then be based on Equation (5), which is re-formulated to account for the displacement of the ship axes due to ship motions:

$$R_{AW}^{lw} = -\frac{\rho\, g}{2} \int_{wl} \overline{\zeta_r^2(x,y,t)}\, n_x\, dl - \omega_e^2\ \Delta\ \overline{\zeta_3\, \zeta_5} + \omega_e^2\ \Delta\ \overline{\zeta_2\, \zeta_6} \qquad (8)$$

where Δ is ship mass.

As wavelength approaches zero, ship motions approach zero but diffraction effects (including wave reflection) become important. SHIPMO uses the following equation adapted from Reference 13 for predicting added resistance in short waves:

$$R_{AW}^{sw} = -\frac{\rho\, g}{2} \int_{wl*} \overline{\zeta_I^2(x,y,t)}\, n_x \times \left\{\sin^2(\theta + \pi - \beta_s) + \frac{2\omega U}{g}\left[1 - \cos\theta\cos(\theta + \pi - \beta_s)\right]\right\} dl \qquad (9)$$

where $wl*$ is the portion of the ship waterline exposed to the incident waves and θ is the horizontal angle between the local waterline and the incident wave direction.

With a strip theory code, no rational method exists for determining added resistance in the transition region between the short and long wave regimes; however, the following equation gives reasonable results using the short and long wave equations:

$$R_{AW} = \begin{cases} R_{AW}^{lw} & \text{for } \lambda/L \geq 1 \\ \max(R_{AW}^{lw}, R_{AW}^{sw}) & \text{for } \lambda/L < 1 \end{cases} \qquad (10)$$

For a ship in irregular seas, the mean added resistance can be evaluated using the following equation from Salvesen [12]:

$$R_{AW} = 2\int_0^\infty \int_{-\pi}^{\pi} R'_{AW}(\beta_s,\omega) S(\beta_s,\omega)\, d\beta_s\, d\omega \qquad (11)$$

where R'_{AW} is added resistance in unit amplitude regular waves and $S(\beta_s,\omega)$ is wave elevation spectral density.

Validation of Added Resistance

For validating added resistance predictions, Strom-Tejsen et al. [16] give experimental data for Series 60 models [17] and O'Dea and Kim [18] give experimental data for an American *FFG 7* frigate. Experimentally determined added resistance is the difference between measured resistance in a seaway and measured resistance in calm water. This difference is typically a small fraction of total resistance;

thus, relative errors in measured added resistance are typically large.

Figure 7 shows comparisons with experiments for the *FFG 7* frigate in head seas. The scatter in the experimental data of Figure 7 is indicative of the uncertainties of added resistance measurements. Comparisons with other experimental values for the *FFG 7* and for Series 60 models indicated accuracy similar to that in Figure 7, with no definite trend for overpredicting or underpredicting experimental results.

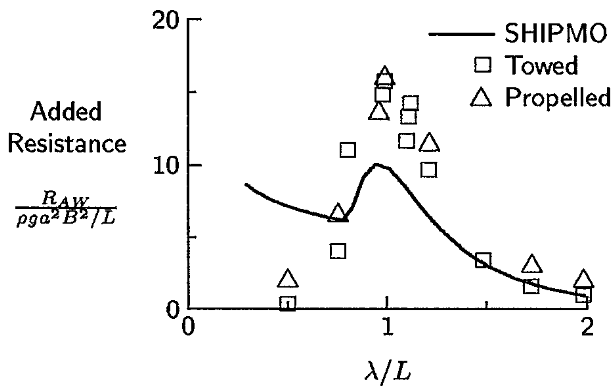

Figure 7: Added Resistance for *FFG 7*, $Fn = 0.30$, Heading = 180 degrees

SEA LOADS INCLUDING APPENDAGE AND VISCOUS FORCES

Sea loads acting on a ship are important for structural design. SHIPMO sea load predictions are based on the theory of Salvesen, Tuck, and Faltinsen [1]. A unique feature of the latest SHIPMO version is that it includes appendage and viscous forces given by Schmitke [3] when evaluating sea loads in the lateral plane.

Past experience with strip theory programs has shown that motion predictions are very good while load predictions are often inaccurate. Consideration of pitch motions and vertical bending moment can provide some insight into this phenomenon. Neglecting heave coupling (typically small), the pitch amplitude of a ship in regular waves can be expressed as:

$$|\zeta_5| = \left| \frac{F_5}{-\omega_e^2 (I_{55} + A_{55}) + i\omega_e B_{55} + C_{55}} \right| \quad (12)$$

where F_5 is excitation force, I_{55} is pitch inertia, A_{55} is added mass, B_{55} is damping, and C_{55} is stiffness. An error of a given percentage in any of the above terms will result in an error of similar percentage in the predicted motion. In contrast, the vertical bending moment at location x along the ship length is:

$$V_5^x = I_5^x - R_5^x - F_5^x - D_5^x \quad (13)$$

where I_5^x is the inertial moment acting forward of x, R_5^x is the hydrostatic moment forward of x, F_5^x if the wave excitation moment forward of x, and D_5^x is hydrodynamic moment due to added mass and damping forward of x. The elements of Equation (13) are complex and of similar magnitude; thus, a relatively small error in any of the terms on the right hand side can produce a large error in the predicted bending moment.

To achieve maximum accuracy for sea load predictions, all forces influencing ship motions and sea loads must be considered in a consistent manner. SHIPMO includes appendage and viscous forces when evaluating motions in the lateral plane; thus, these forces must also be included when evaluating sea loads. For predicting sea loads, Reference 1 includes hydrodynamic end-effect terms. Consequently, motion predictions must also include end-effect terms. Consistency is also required for numerical methods used for integrating motion and sea load forces along the length of the ship. For hydrodynamic and hydrostatic forces, Simpson's rule gives good results for numerical integration. For inertial forces, Simpson's rule becomes less reliable because it is not suited to large variations in inertia that can occur along the length of a ship. Instead, SHIPMO uses a rectangular rule for integrating inertia, with the assumption that inertia is uniformly distributed between mid-stations (e.g. the mass of station 2 is uniformly distributed between stations 1.5 and 2.5).

Input Ship Inertia Properties

Predicting sea loads on a ship requires input inertia properties for each section along the ship length. For most ships, the longitudinal mass distribution is known to acceptable accuracy. Estimates of the vertical centre of gravity are also typically known for ship sections; however, sectional roll gyradii are typically unknown. To circumvent this problem, SHIPMO uses the following procedure to estimate sectional roll gyradii:

1. Calculate roll moment of inertia I_{44} for the entire vessel using an input roll radius of gyration r_{xx}:

$$I_{44} = \triangle\, r_{xx}^2 \quad (14)$$

2. Assume that the local roll gyradius r_{xx-i} about the sectional CG is directly proportional to the square root of the mass per unit length m_i/l_i of the section. This assumption is based on the premise that the mass for each section can be modelled as a circular cylinder, with density being constant along the entire ship length but with a different radius for each ship section. A single proportionality constant k_r is applicable along the length of the ship.

$$r_{xx-i} = k_r \sqrt{\frac{m_i}{l_i}} \tag{15}$$

3. Solve for the proportionality constant k_r. The following equation gives the total roll inertia of the ship:

$$I_{44} = \sum_{i=1}^{N_s} \left(k_r^2 \frac{m_i}{l_i} + z_i^2 \right) m_i \tag{16}$$

where N_s is the number of ship sections and z_i is the sectional CG elevation relative to the ship CG. Using the above equation, the constant k_r is solved as follows:

$$k_r = \sqrt{\frac{I_{44} - \sum_{i=1}^{N_s} m_i z_i^2}{\sum_{i=1}^{N_s} \frac{m_i^2}{l_i}}} \tag{17}$$

4. Compute the sectional roll gyradii using Equation (15).

This method provides reasonable estimates of sectional roll gyradii which are consistent with the ship inertia properties. In practice, the ship roll natural frequency is often known and provided as input for SHIPMO to compute the ship roll inertia using the following relationship:

$$\omega_4 = \sqrt{\frac{\overline{GM}\, \Delta\, g}{\Delta r_{xx}^2 + A_{44}}} \tag{18}$$

where ω_4 is roll natural frequency, $\overline{GM}$ is metacentric height, and A_{44} is computed roll added mass. For a naval frigate, the roll added mass of the hull and appendages is typically 20 percent of the dry roll inertia.

For accurate load predictions, the ship inertial properties used for computing ship motions (e.g. ship mass, roll gyradius, and pitch gyradius) must be consistent with the inertial properties based on input sectional distributions. The ship mass and longitudinal centre of gravity (LCG) must also be consistent with the displacement and longitudinal centre of buoyancy based on hydrostatics. SHIPMO provides output to assist checking ship inertial properties. In practice, the user often provides the ship mass and LCG as input to SHIPMO, which then computes appropriate ship draft and trim. The resulting draft and trim usually differ slightly from the actual values; however, these slight differences are insignificant relative to the importance of having consistent inertial properties.

VALIDATION OF SHIP MOTIONS AND SEA LOADS

The new version of SHIPMO has been extensively validated using open literature data for a warship model from Lloyd, Brown, and Anslow [10, 11] and proprietary data for a Canadian Patrol Frigate (CPF). This paper gives some results for the warship model, while some additional results for the CPF can be found in the paper by McTaggart et al. [19]. The warship data of Lloyd et al. are the most complete experimental data of ship motions and sea loads available in the open literature. Figure 8 shows the waterplane of the warship, which has a slender geometry including a narrow stern; thus, strip theory should be able to give good predictions for this ship.

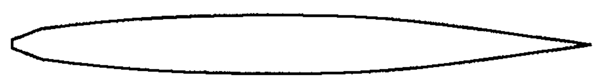

Figure 8: Warship Model Waterplane

A critical test for sea load predictions is that all loads must be zero at either end of the ship. In SHIPMO, sea loads are obtained through integration of forces forward of the station in question; thus, computed sea loads at the aft end of the ship will reveal any inconsistencies between forces used for ship motions and sea loads. SHIPMO correctly gives zero sea loads at the aft end of the ship for all modes.

For vertical plane motions and sea loads, results for the warship in head seas at a Froude number of 0.21 are presented here. Figures 9 and 10 show good agreement between experimental and predicted heave and pitch motions. Figure 11 shows similarly good agreement for bending moment at midships. The experimental data for vertical shear at station 5 in Figure 12 show significant scatter; however, SHIPMO matches the data trends.

For lateral plane motions and sea loads, warship

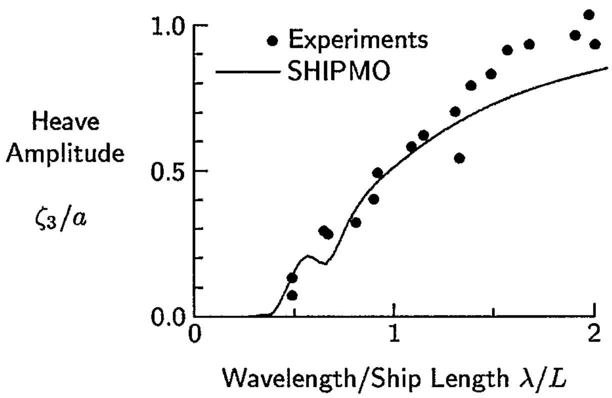

Figure 9: Warship Heave Amplitude in Regular Head Waves, $Fn = 0.21$

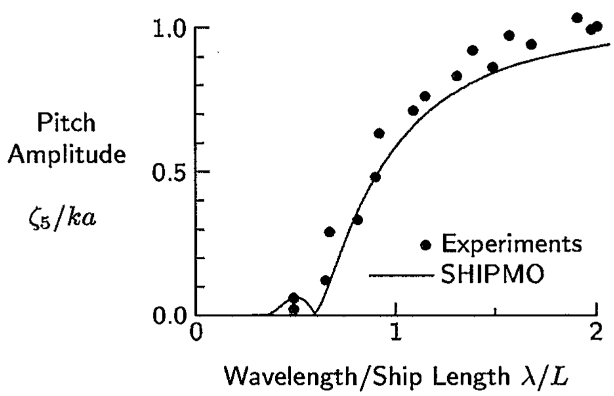

Figure 10: Warship Pitch Amplitude in Regular Head Waves, $Fn = 0.21$

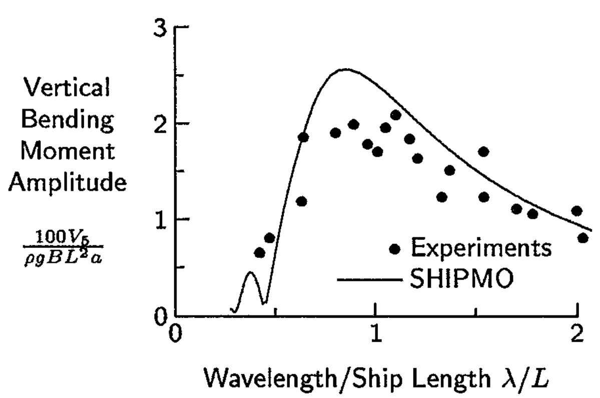

Figure 11: Warship Vertical Bending Moment at Midships in Regular Head Waves, $Fn = 0.21$

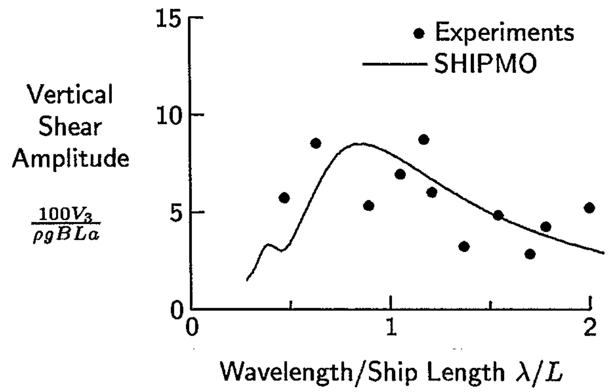

Figure 12: Warship Vertical Shear at Station 5 in Regular Head Waves, $Fn = 0.21$

results are presented for a Froude number of 0.21 and heading of 30 degrees because this is one of the few cases for which complete experimental data are available. Computations are given for both an appended ship and unappended ship, with the dry roll gyradius being constant. The roll and yaw motions are given in Figures 13 and 14 and horizontal bending moment and torsion at midships are given in Figures 15 and 16. The predicted roll, yaw, and horizontal bending moment are in good agreement with the experimental results, with inclusion of appendage forces giving better results. For torsion, SHIPMO overpredicts torsion when appendages are included. Errors in predicted torsion are likely due to uncertainties in the roll inertia properties of the warship model segments, as discussed in References 10 and 11.

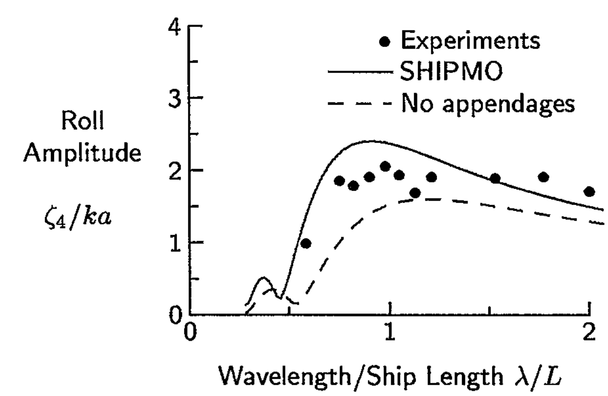

Figure 13: Warship Roll in Stern Quartering Seas, $\beta_s = 30$ Degrees, $Fn = 0.21$

Results for the CPF reported in Reference 19 were not quite as good as those shown here. The difference in accuracy is attributed to the transom

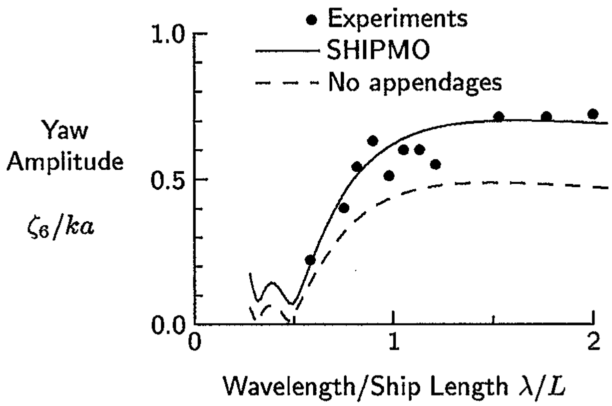

Figure 14: Warship Yaw in Stern Quartering Seas, $\beta_s = 30$ Degrees, $Fn = 0.21$

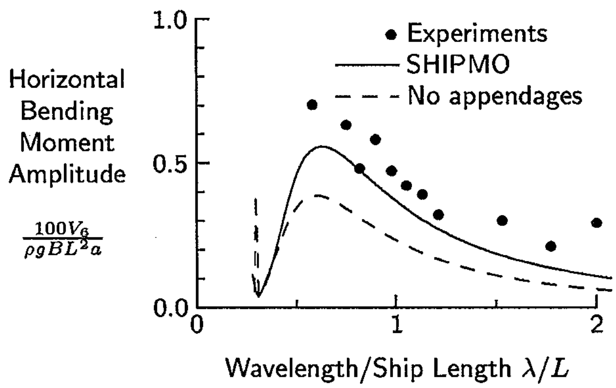

Figure 15: Warship Horizontal Bending Moment at Midships in Stern Quartering Seas, $\beta_s = 30$ Degrees, $Fn = 0.21$

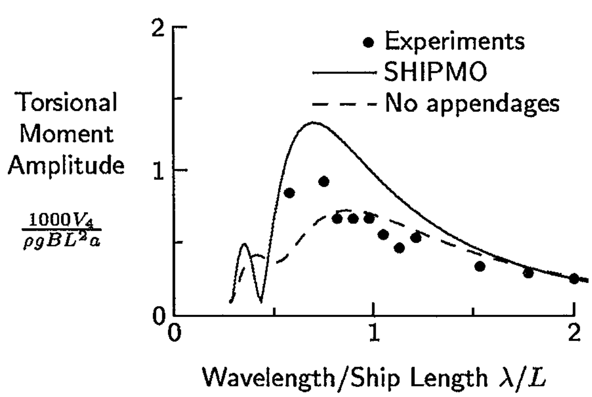

Figure 16: Warship Torsional Bending Moment at Midships in Stern Quartering Seas, $\beta_s = 30$ Degrees, $Fn = 0.21$

stern of the CPF, which violates the strip theory assumption that longitudinal variations in section shape are small.

CONCLUSIONS

The new version of the strip theory program SHIPMO includes several features to enhance its robustness. A new boundary element method eliminates sectional irregular frequencies, a common problem with the Frank close-fit method. Approximations based on zero and infinite frequency limits for sectional coefficients give reliable results at low and high encounter frequencies. At very low encounter frequencies, SHIPMO uses an extrapolation scheme to circumvent inherent theoretical limitations with strip theory.

The new version of SHIPMO includes added resistance and sea loads capabilities. Although added resistance is difficult to predict because it is a second-order effect, SHIPMO gives acceptable agreement with experiments. The updated sea loads capability includes the influence of viscous and appendage forces in the lateral plane. Comparisons with experiments for a warship model show good agreement for motions, bending moments, and vertical shear. Differences between predicted and experimental torsional moments are likely due to uncertainties regarding the roll inertial distribution of the model.

REFERENCES

[1] N. Salvesen, E.O. Tuck, and O. Faltinsen, "Ship Motions and Sea Loads," *Transactions, Society of Naval Architects and Marine Engineers* **78**, 250–287 (1970).

[2] J.D. Howard, S.M. Calisal, and L. Barnard, "Seakeeping Evaluation of a Low L/B Hull Form Series," in *Proceedings of the Third Canadian Marine Hydrodynamics and Structures Conference* (Dartmouth, Nova Scotia, August 1995), pp. 125–135.

[3] R.T. Schmitke, "Ship Sway, Roll, and Yaw Motions in Oblique Seas," *Transactions, Society of Naval Architects and Marine Engineers* **86**, 26–46 (1978).

[4] Y. Himeno, "Prediction of Ship Roll Damping - State of the Art," Report 239, Department of Naval Architecture and Marine Engineering, University of Michigan, 1981.

[5] W. Frank, "Oscillation of Cylinders on or Below the Free Surface of Deep Fluids," Report 2305, Naval Ship Research and Development Center, October 1967.

[6] P.D. Sclavounos and C. Lee, "Topics on Boundary Element Solutions of Wave Radiation-Diffraction Problems," in *Fourth International Conference on Numerical Ship Hydrodynamics* (Washington, 1985).

[7] J.N. Newman, "The Evaluation of Free-Surface Green Functions," in *Fourth International Conference on Numerical Ship Hydrodynamics* (Washington, 1985).

[8] J.N. Newman, *Marine Hydrodynamics*, MIT Press, Cambridge, Massachusetts, 1977.

[9] W.D. Kim, "On the Harmonic Oscillations of a Rigid Body on a Free Surface," *Journal of Fluid Mechanics* **21** (1965).

[10] A.R.J.M. Lloyd, J.C. Brown, and J.F.W. Anslow, "Motions and Loads on Ship Models in Regular Oblique Waves," *Transactions, Royal Institution of Naval Architects* **122**, 21–43 (1980).

[11] A.R.J.M. Lloyd, J.C. Brown, and J.F.W. Anslow, *Wave Induced Motions and Loads on a Model Warship*, Royal Institution of Naval Architects, Occasional Publication No. 3, 1980.

[12] N. Salvesen, "Added Resistance of Ships in Waves," *Journal of Hydronautics* **12**(1), 24–34 (1978).

[13] O.M. Faltinsen, K.J. Minsaas, N. Liapis, and S.O. Skjordal, "Prediction of Resistance and Propulsion of a Ship in a Seaway," in *Thirteenth Symposium on Naval Hydrodynamics* (Tokyo, 1980), pp. 505–529.

[14] G.E. Hearn, K.C. Tong, and S.M. Lau, "Hydrodynamic Models and their Influence on Added Resistance Predictions," in *PRADS '87 - The Third International Symposium on Practical Design of Ships and Mobile Units* (Trondheim, Norway, June 1987), Vol. 3, pp. 302–316.

[15] J.J. Blok and J. Huisman, "Relative Motions and Swell-Up for a Frigate Bow," *Transactions, Royal Institution of Naval Architects* **126**, 227–244 (1984).

[16] J. Strom-Tejsen, H.Y.H. Yeh, and D.D. Moran, "Added Resistance in Waves," *Transactions, Society of Naval Architects and Marine Engineers* **81**, 109–143 (1973).

[17] F.H. Todd, "Some Further Experiments on Single-Screw Merchant Ship Forms - Series 60," *Transactions, Society of Naval Architects and Marine Engineers* **61**, 516–589 (1953).

[18] J.F. O'Dea and Y.H. Kim, "Added Resistance and Power of a Frigate in Regular Waves," Report DTNSRDC/SPD-0964-02, DTNSRDC, September 1981.

[19] K. McTaggart, I. Datta, A. Stirling, S. Gibson, and I. Glen, "Motions and Loads of a Hydroelastic Frigate Model in Severe Seas," *Transactions, Society of Naval Architects and Marine Engineers* **105** (1997).

#503454